PROTECTED
CANMET

ANDI-23

ATOMIC ENERGY OF CANADA LIMITED

NEUTRON DIFFRACTION MEASUREMENTS OF CRYSTALLOGRAPHIC TEXTURE IN SINGLE-PASS WELD AND T-WELD MATERIAL
(Part of the Program of the Federal Panel on Energy R & D [PERD])

T.M.Holden and J.H. Root

Abstract

The crystallite orientation distribution functions for a sample of weld metal taken from a single-pass weld, for a sample taken from the plate in which the weld was deposited and for the construction material of a T-weld have been obtained from neutron diffraction measurements. The principal grain orientations are identified and discussed. With a knowledge of the appropriate single crystal elastic constants, the effective Young's modulus as a function of orientation has been computed from the distribution function for each sample.

Neutron and Solid State Physics Branch
Atomic Energy of Canada Limited
Chalk River Nuclear Laboratories
Chalk River, Ontario, K0J 1J0, Canada
1989 March

Work on the project was conducted under the auspices of the Canada Centre for Mineral and Energy Technology, Energy, Mines and Resources Canada

DSS File No: 007SQ.23440-8-9208
DSS Contract Serial No. 23440-8-9208/01SQ
CANMET Scientific Authority: Mr. G. Roy

MICROMEDIA

20 pp

Introduction

The intensity of a diffraction peak from a polycrystalline sample depends on the scattering angle, the structure factor, the multiplicity of the reflection, the geometry of the sample and its effective absorption, the geometry of the spectrometer and the volume fraction of grains whose (hkl) plane normals lie along the scattering vector. If the sample orientation is stepped systematically in tilt and rotation over a hemisphere at the scattering angle for the (hkl) reflection, a quantity proportional to the volume fraction of grains with plane normals in a given direction may be mapped out and presented in the form of a pole-figure. The structure observed in the pole-figure is called the crystallographic texture. Analysis of the pole-figures for a number of (hkl) reflections permits the determination of the crystallite orientation distribution function (CODF) via the surface harmonic method described by Roe[1,2]. A computer code to do this has been written[3] and checked at Chalk River Nuclear Laboratories.

The CODF is defined uniquely in terms of generalized harmonics in the three Euler angles (ψ,θ,ϕ) shown in Fig. 1d by the series expansion[2]

$$\omega(\zeta,\psi,\phi) = \Sigma_{l=0}^{\infty} \Sigma_{m=-l}^{l} \Sigma_{n=-l}^{l} W_{lmn} Z_{lmn}(\zeta) e^{-im\psi} e^{-in\phi}, \qquad (1)$$

where Z_{lmn} are generalized Lengendre functions[2] and $\zeta = \cos\theta$. The set of coefficients W_{lmn}, determined from the pole figures, completely specifies the distribution function. The volume fraction of crystallites with coordinate axes (XYZ) oriented between (θ,ψ,ϕ) and $(\theta + d\theta, \psi + d\psi, \phi + d\phi)$ with respect to the coordinate axes (xyz) of the sample is $\omega(\theta,\psi,\phi)\sin\theta d\theta d\psi d\phi$.

Three sets of measurements are reported here; the average texture of the weld metal deposited in a V-groove in a stainless alloy plate, the average texture in the plate material directly under the V-groove and the average texture of the construction material of a T-weld. Neutron diffraction measurements of residual strain have been reported for both the stainless steel plate[4] and the T-weld[5]. The crystallite orientation distribution functions have been used to calculate the directional dependence of Young's modulus for each of the three materials studied.

Experiments

(a) Samples

(i) Stainless Steel Plate

The material of the plate was 316 L stainless steel and had nominal composition (wt%) $Cr_{18}Ni_{14}Mo_2Mn_2Si_1Fe_{63}$. The weld was deposited along a V-groove in the plate by the submerged arc method by the Welding Section of the Physical Metallurgical Research Laboratory of the Ministry of Energy, Mines and

Resources, Ottawa. The mean intercept grain size corrected for the existence of annealing twins was 0.053 mm and the grains were equiaxed. The relatively large grain size would be a considerable draw-back for X-ray texture measurements since there would be only a few correctly oriented grains in the volume of overlap of the incident and scattered X-ray beams. This is alleviated in our neutron experiments by using a 20 mm high, 5 mm diameter sample fully bathed in the neutron beam. One sample was cut from the weld metal deposited in the groove, and one sample was taken from the plate material just under the groove. Figure 1(a) shows the Cartesian coordinate axes chosen to describe the weld metal. The plate normal, N, is designated x, the direction in the plate transverse (T) to the weld is designated y and the direction along the single-pass weld is designated z. The Cartesian coordinate axes chosen to describe the sample under the V-groove are the same as for the weld metal and are shown in Fig 1b.

(ii) Construction Material for the T-Weld

The 25.4 mm plate was fabricated to Lloyds LT60 specifications and had nominal composition (wt%) $C_{0.14}Mn_{1.47}P_{0.01}Si_{0.25}Ni_{0.27}Mo_{0.01}V_{0.07}Nb_{0.02}Ti_{0.006}$ $Al_{0.02}Fe_{97.7}$. Figure 1c shows how a cylindrical sample was cut from a piece of the base plate. The x-axis is taken to be parallel to the rolling direction (RD) of the plate, the y-axis is transverse (TD) to the rolling direction in the plane of the plate and the z-axis is parallel to the plate normal (N).

(b) Neutron Diffraction

The experiments were carried out on the L3 spectrometer at the NRU reactor, Chalk River, operated as a diffractometer with an incident-neutron wavelength of 1.5446 Å provided by a Ge (113) monochromator. The collimation before and after the sample was 1°. The sample was rotated over a hemisphere in steps of 5° in tilt and rotation by means of a computer controlled goniometer for each of the three scattering angles for (111), (002) and (220) reflections for the stainless steel weld and the plate material and (110), (002) and (112) for the T-weld plate material. The diffuse background, obtained by offsetting the scattering angle from a Bragg angle, was measured separately and subtracted from the Bragg scattering. The variation of the diffuse scattering with the angle of tilt gives an experimental measure of the variation of the effective absorption of the sample. This geometrical correction was applied to the diffraction data.

Results

The (111), (002) and (220) pole figures for the sample of weld metal from the single-pass weld are presented in Fig. 2. The result at the top of each pole figure represents the texture in the x-direction, i.e. the normal to the plate. The result at the left represents the texture in the y-direction which is transverse to the weld, while the result at the centre represents the texture along the weld. As indicated in Fig. 2, η is the azimuthal angle from the x-direction while χ is the tilt from the z-direction. Very strong orientation effects are clearly present since the texture coefficients are as high as ten

effects are clearly present since the texture coefficients are as high as ten times random. The grains in the weld are aligned with <001> axes along the weld direction and perpendicular to the sides of the V-groove and with <110> axes in the normal and transverse directions. The coefficients of the generalized harmonics describing the orientation distribution function[1,2] are tabulated with errors in Table 1. The $\phi = 45°$ section through the Euler space described by angles (ψ,θ,ϕ) for describing the grain orientation (Fig. 1d) is shown in Fig. 3. Comparison with charts prepared by Davies, Goodwill and Kallend[6] allows identification of the principal orientation (001) [110], i.e. the orientation in which the z-axis is normal to the (001) plane and the x-axis is a [110] direction. There is a less important region of intensity near $\theta = 90$, $\psi = 50°$ corresponding to ideal orientations of (110) [111] and (110) [223]. The former puts (220) intensity in the normal direction and at 54.7° from the transverse direction in the xy plane. The latter puts (111) intensity 11° from the normal and 8° from the transverse direction.

The solidification of grains in the melt pool proceeds with {100} planes normal to the direction of principal heat flow out of the pool. This direction is mainly directed from the centre of the pool to the sides of the V-groove. This fact accounts for the {001} grain orientation being predominantly along the bisector of the x and y directions.

The (111), (002) and (220) pole figures for the sample of 316 L stainless steel taken from below the V-groove are shown in Fig. 4. The texture is much less pronounced than in the weld metal and the maximum texture coefficient is 1.8. The principal features are a strong orientation component with (111) plane normals along the transverse direction, y, which is the rolling direction of the plate and (220) plane normals about 30° from the z-direction in the xz plane. The coefficients of the orientation distribution function are given in Table 2 and the $\phi = 45°$ section in Euler space is shown in Fig. 5. The principal orientation ($\psi = 90$, $\theta = 35$, $\phi = 45$) corresponds to the ideal orientation[6] (112) [110]. The z axis is normal to the (112) plane and is therefore designated by [112] and the x axis is aligned along the [110] direction thus giving a peak at the top of the (220) pole figure, and peaks from the {220} reflection 30° from the longitudinal direction. The y-axis, the rolling direction of the plate, is aligned along the [111] direction for the principal orientation.

The (110), (002) and (112) pole figures from the T-weld base plate material are shown in Fig. 6. The texture is again weak, with a maximum texture coefficient of 1.7. The principal features of the (110) pole figure are the maxima in the rolling direction (x) and approximately 30° from the normal direction in the plane containing the normal (z) and the rolling direction (x). The principal features of the (002) pole figure are a peak along the normal direction and peaks 60° from the normal in the plane containing the normal and the rolling direction. The coefficients describing the orientation distribution function are given in Table 3 and the $\phi = 45°$ section in Euler space is shown in Fig. 7. The line $\psi = 90°$ in the $\phi = 45°$ section is known as the [110] fibre axis since it includes several ideal orientations with a [110] axis along the rolling direction while the rolling plane can be one of several planes. Likewise the

line $\theta = 54.7°$ is known as the $(\bar{1}11)$ fiber axis because it corresponds to a rolling plane $(\bar{1}11)$ with one of several orientations in that plane along the rolling direction. Basically the weight in Fig. 7 is concentrated in a reversed L-shaped ridge including these axes. Similar effects have been observed[7,8] in successively deformed cold-rolled steels. The ideal orientations enclosed by the largest contour, 1.8 times random, include the (001) $[\bar{1}\bar{1}0]$, $(\bar{1}13)$ $[\bar{1}\bar{1}0]$ and $(\bar{1}12)$ $[\bar{1}\bar{1}0]$ orientations. The first of these accounts for the peak in the normal direction in the (002) pole figure while the second and third put intensity close to 30° from the normal direction in the xz plane. There is also extra intensity at $\psi = 0$, $\theta = 60$ which corresponds to the ideal orientations $(\bar{1}11)$ $[1\bar{1}2]$ and $(\bar{5}54)$ $[2\bar{2}5]$.

Calculations of Young's Modulus

The reciprocal of Young's modulus in a cubic single crystal varies with orientation as follows[9]

$$\frac{1}{E} = S_{11} - 2\,(S_{11} - S_{12} - 0.5\,S_{44})\,(\alpha_1^2\alpha_2^2 + \alpha_2^2\alpha_3^2 + \alpha_3^2\alpha_1^2) \qquad (2)$$

where α_1, α_2, α_3 are direction cosines with respect to the crystal coordinate system (XYZ) and S_{ij} are single crystal compliance constants whose values are given in Table 4. The crystallite orientation distribution function enables us to calculate the effective Young's modulus as a function of orientation in the polycrystalline samples. Equation (2) can be written as a function, $f(\theta,\phi)$, in angles specifying direction with respect to crystal axes.

The average reciprocal of Young's modulus, $\langle 1/E\rangle_{\chi,\eta}$, is the integral of $f(\theta,\phi)$ weighted by the probability, $h_{\chi,\eta}(\theta,\phi)$, that a particular crystal direction (θ,ϕ) is pointing along sample direction (χ,η).

$$\langle 1/E\rangle_{\chi,\eta} = \int_0^{2\pi} d\phi \int_0^{\pi} d\theta\, \sin\theta\, f(\theta,\phi)\, h_{\chi,\eta}(\theta,\phi) \qquad (3)$$

The probability distribution is obtained from W_{lmn}, the expansion coefficients by means of which the CODF is represented as a series of generalized harmonic functions, and $P_{ln}(x)$, the normalized associated Legendre polynomials of Roe [2].

$$h_{\chi,\eta}(\theta,\phi) = \sum_{lmn} [8\pi^2/(2l+1)]^{1/2}\, W_{lmn} P_{lm}(\cos\chi) e^{-im\eta}\, P_{ln}(\cos\theta) e^{in\phi} \qquad (4)$$

For cubic materials, only fourth order terms appear in a harmonic expansion of 1/E so that only the W_{lmn} terms of fourth order are required for a calculation of $\langle 1/E\rangle$ in a particular direction.

The results for the weld metal, for the stainless steel sample taken from under the V-groove and for the T-weld base material are shown as pole figures in Figs. 8-10 with contours labelled by the factor by which the effective value of Young's modulus exceeds the value calculated for zero crystallographic texture. In the weld metal, Fig. 8, the material is stiffest in the normal, x, and transverse, y, directions and softest in directions perpendicular to the V-groove surface and along the weld. In total there is a 20% variation in Young's modulus as a result of the very marked texture. In the base metal, Fig. 9, the effects are much less marked with a 1.6% overall variation. The stiffest direction corresponds to the rolling direction, y, of the plate In the bcc T-weld base material the stiffest direction is again the transverse direction although the maximum to minimum variation is only 1.0%.

It would be interesting to make measurements of the elastic properties of the weld metal in different directions in order to check the predictions of the calculations of Young's modulus.

References

1. R.-J. Roe, J. Appl. Phys. 36, 2024 (1965).
2. R.-J. Roe, J. Appl. Phys. 37, 2069 (1966).
3. J.H. Root and T.M. Holden, Atomic Energy of Canada Limited Report, ANDI-29 (1989).
4. T.M. Holden, J.H. Root, V. Fidleris, R.A. Holt and G. Roy, Materials Forum, 27-28, 359 (1988).
5. T.M. Holden, J.H. Root, R.A. Holt and G. Roy. Proceedings of the Seventh International Conference on Offshore Mechanics and Arctic Engineering, Vol. III p. 127. Edited by M.M. Salama, R. Denys, H.C. Rhee and J.Y. Koo. (The American Society of Mechanical Engineers: New York) 1988.
6. G.J. Davies, D.J. Goodwill and J.S. Kallend, J. Appl. Cryst. 4, 67 (1971).
7. A.J. Heckler and W.G. Granzow, Metall. Trans. 1, 2089 (1970).
8. S. Misra and C. Darmann, Int. Metals Reviews 6, 307 (1982).
9. J.F. Nye, "Physical Properties of Crystals" (Clarendon Press: Oxford) 1985.

Table 1

Low order coefficients W_{lmn} describing the orientation distribution function for the weld-metal. Units of 10^{-4}.

$W_{000} = 179.1$

$W_{400} = 105.9 \pm 5.2$

$W_{420} = 0.0 \pm 0.7$

$W_{440} = -88.9 \pm 2.5$

$W_{600} = -6.9 \pm 2.5$

$W_{620} = -8.7 \pm 0.1$

$W_{640} = 14.6 \pm 1.3$

$W_{660} = 10.0 \pm 0.9$

$W_{800} = 56.2 \pm 1.1$

$W_{820} = -5.6 \pm 0.7$

$W_{840} = -33.5 \pm 1.9$

$W_{860} = -27.0 \pm 1.0$

$W_{880} = 50.2 \pm 2.5$

Table 2

Low order coefficients W_{lmn} describing the orientation distribution for the stainless steel plate. Units of 10^{-4}.

$W_{000} = 179.1$

$W_{400} = 2.7 \pm 5.2$

$W_{420} = -6.6 \pm 1.0$

$W_{440} = -3.0 \pm 0.6$

$W_{600} = 5.3 \pm 1.9$

$W_{620} = -7.2 \pm 0.1$

$W_{640} = -3.3 \pm 0.1$

$W_{660} = -2.2 \pm 0.1$

$W_{800} = 3.7 \pm 1.4$

$W_{820} = -0.5 \pm 0.3$

$W_{840} = 3.1 \pm 0.2$

$W_{860} = 1.0 \pm 0.2$

$W_{880} = -0.3 \pm 0.2$

Table 3

Low order coefficients W_{lmn} describing the orientation distribution function for the base material for the T-weld. Units of 10^{-4}.

$W_{000} = 179.1$

$W_{400} = -0.6 \pm 1.6$

$W_{420} = -5.0 \pm 0.7$

$W_{440} = -2.6 \pm 1.0$

$W_{600} = 14.1 \pm 0.1$

$W_{620} = -12.7 \pm 0.3$

$W_{640} = 6.8 \pm 0.6$

$W_{660} = 0.5 \pm 0.9$

$W_{800} = -1.8 \pm 0.2$

$W_{820} = 1.8 \pm 0.2$

$W_{840} = -0.7 \pm 0.3$

$W_{860} = -0.6 \pm 0.4$

$W_{880} = 1.2 \pm 0.2$

Table 4

Single crystal elastic compliance constants (Units $10^{-3}GPa^{-1}$)

Material	S_{11}	S_{12}	S_{44}
Iron[a]	7.563	-2.788	8.547
Stainless steel[b]	9.85	-3.84	7.68

a. D.J. Dever, J. Appl. Phys. 43. 3293 (1972).
b. The average of the single crystal elastic constants for 18-12 stainless steel obtained by three groups of workers: M. Kikuchi, Transactions of Japan Institute of Metals 12, 417 (1971). G. Bradfield, J. of the Iron and Steel Institute, 202, 616 (1964). M.C. Mangalick and N.F. Fiore, Trans. Metall. Soc. Am. Inst. Mech. Eng., 242, 2363 (1968).

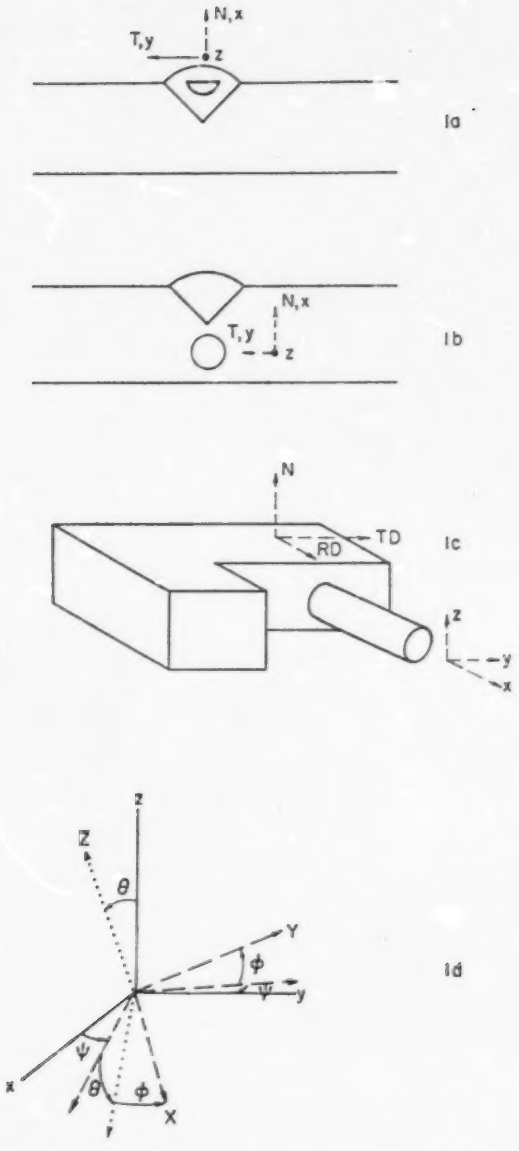

Fig. 1. Geometrical arrangement of the samples taken from the single pass weld including the Cartesian systems used to specify sample orientation (Figs. 1a and 1b). Geometrical arrangement of the sample taken from the T-weld showing rolling, transverse and normal directions and the Cartesian axes (Fig. 1c). Euler angle system (ψ,θ,ϕ) describing crystal orientation XYZ in the sample system xyz (Fig. 1d).

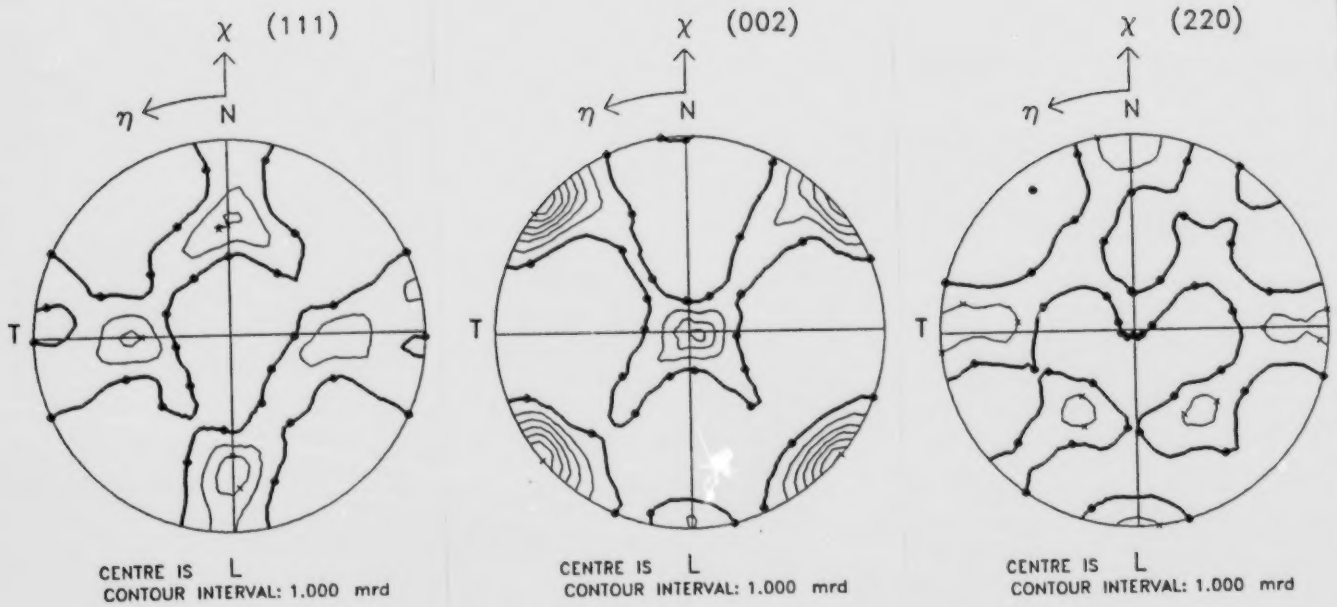

Fig. 2. (111), (002) and (220) pole figures for the sample taken from the weld metal of the single pass weld. The heavy contour in each corresponds to a random texture. Solid contour lines indicate increasing texture with a contour interval of 1.0 of the random texture: i.e., 2, 3 etc. times the random texture. The decorated contours indicate maximum and minimum textures.

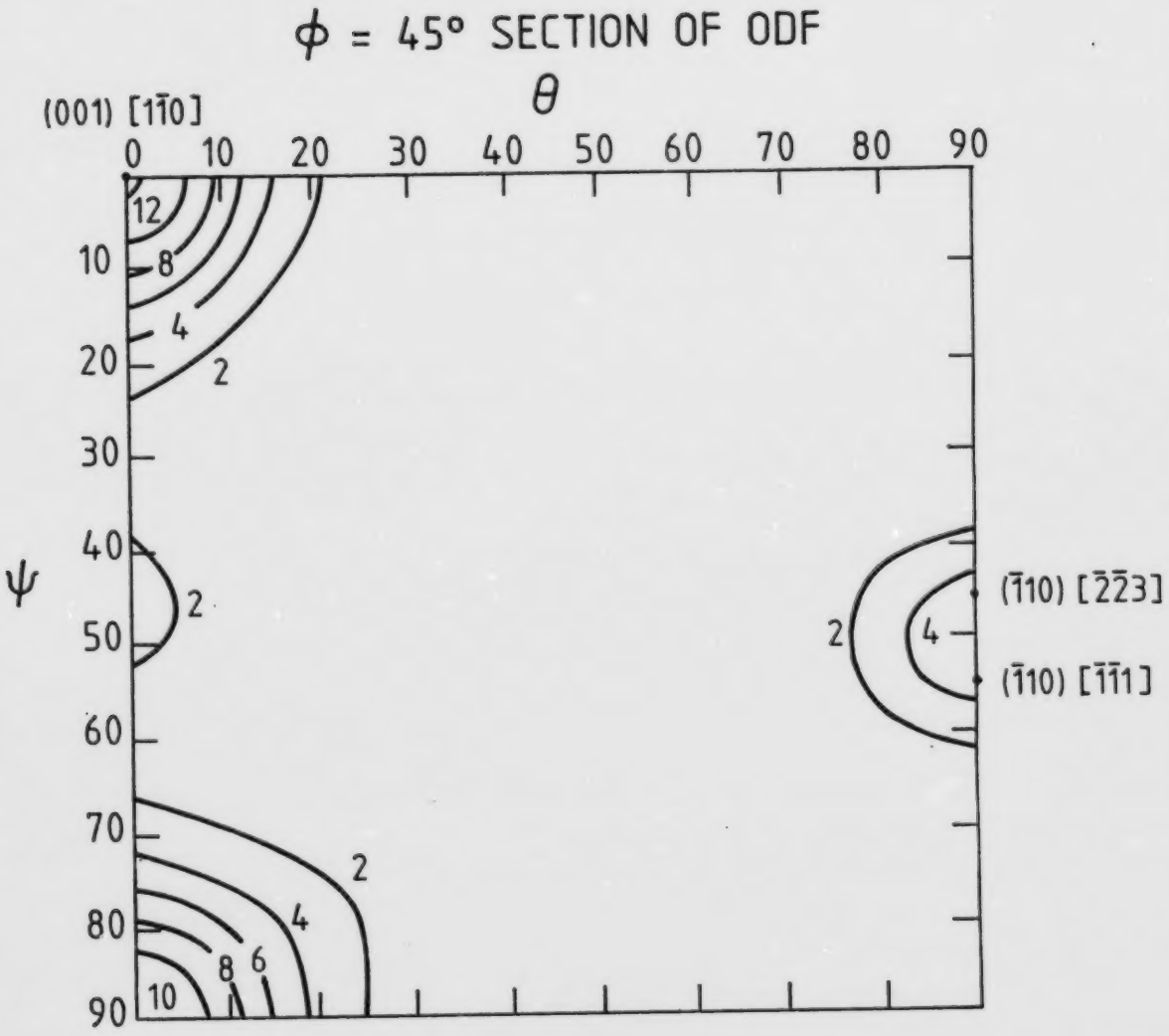

Fig. 3. ϕ = 45° section of the orientation distribution function for the sample of weld metal from the single-pass weld. The positions of several particular crystal orientations are indicated. The contours are labelled by the factor by which the grain orientation departs from a random orientation.

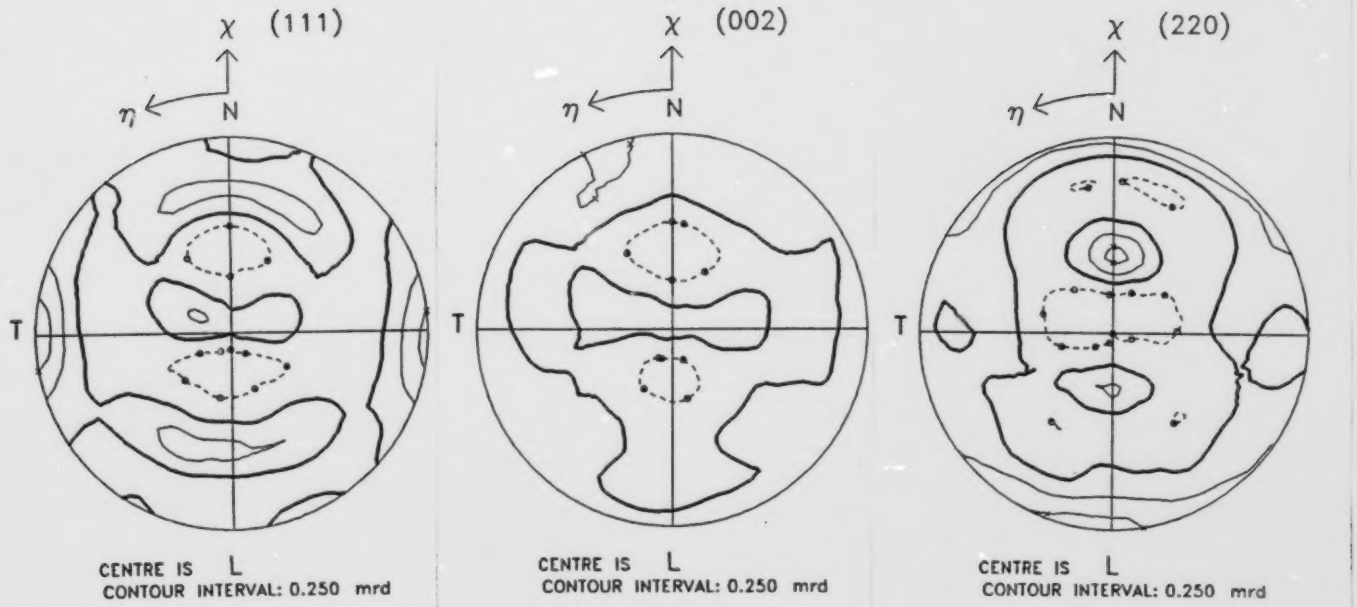

Fig. 4. (111), (002) and (220) pole figures for the sample taken below the weld in a single-pass weld. The heavy contour in each pole figure corresponds to random texture. Solid contour lines indicate increasing texture with a contour internal of 0.25 of the random texture: i.e., 1.25, 1.5 etc. times the random texture. Dashed lines indicate decreasing texture. Decorated contours indicate maximum and minimum textures.

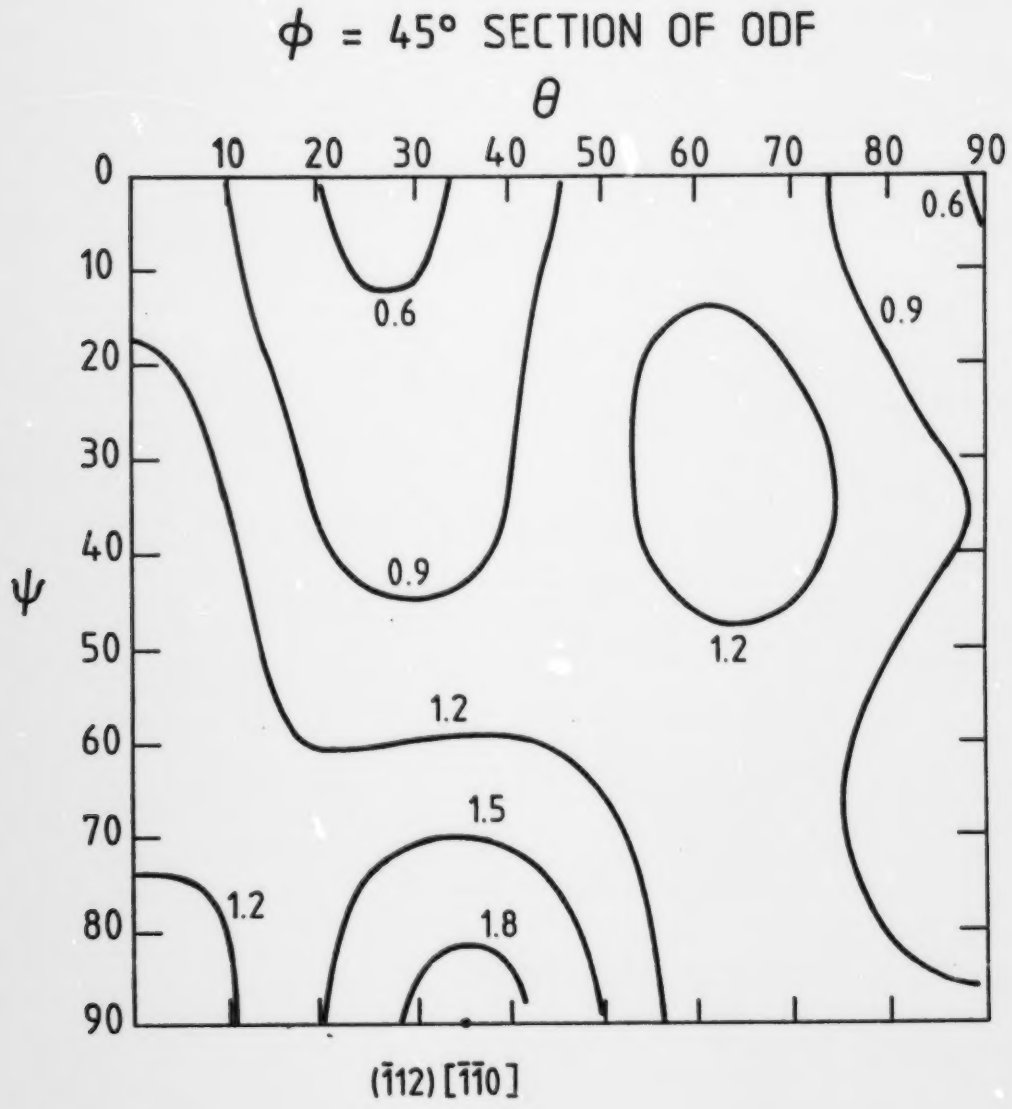

Fig. 5. ϕ = 45° section of the orientation distribution function for the sample taken below the weld. While there is a wide distribution of orientations, the most prominent orientation is (112) [110]. The contours are labelled by the factor by which the grain orientation departs from a random orientation.

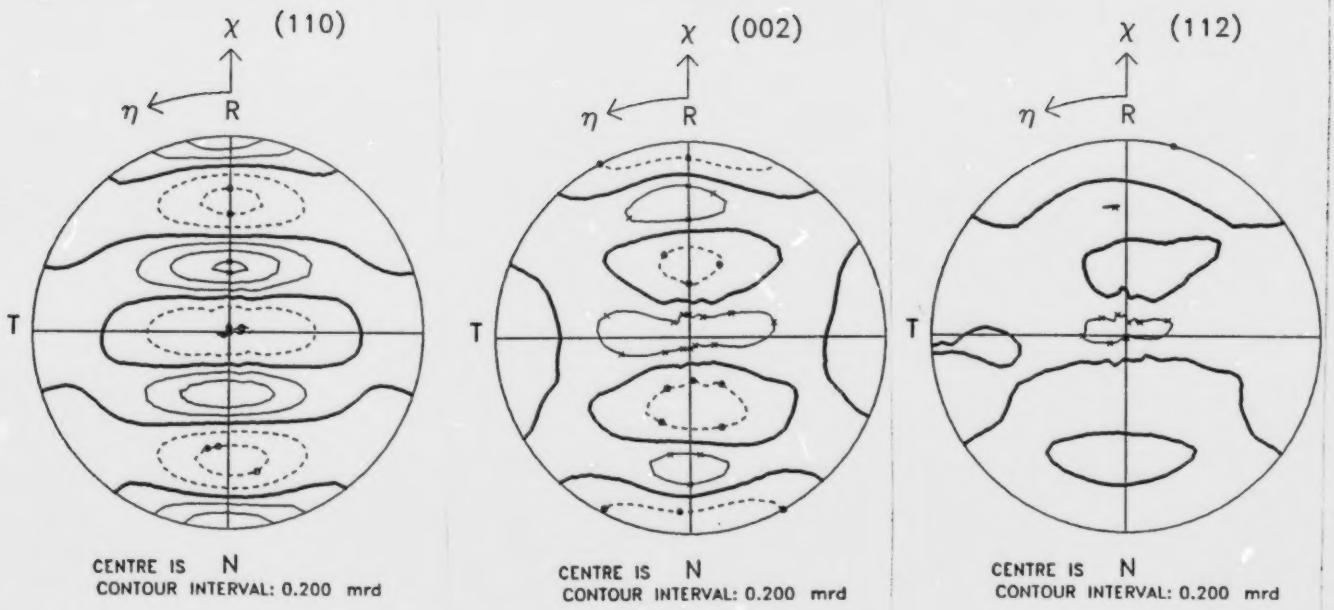

Fig. 6 (110, (002) and (112) pole figures for the T-weld sample. The heavy contour in each pole figure corresponds to random texture. Solid contour lines indicate increasing texture with a contour interval of 0.2 of the random texture: i.e., 1.2, 1.4 etc. times the random texture. Dashed lines indicate decreasing texture. Decorated contours indicate maximum and minimum textures.

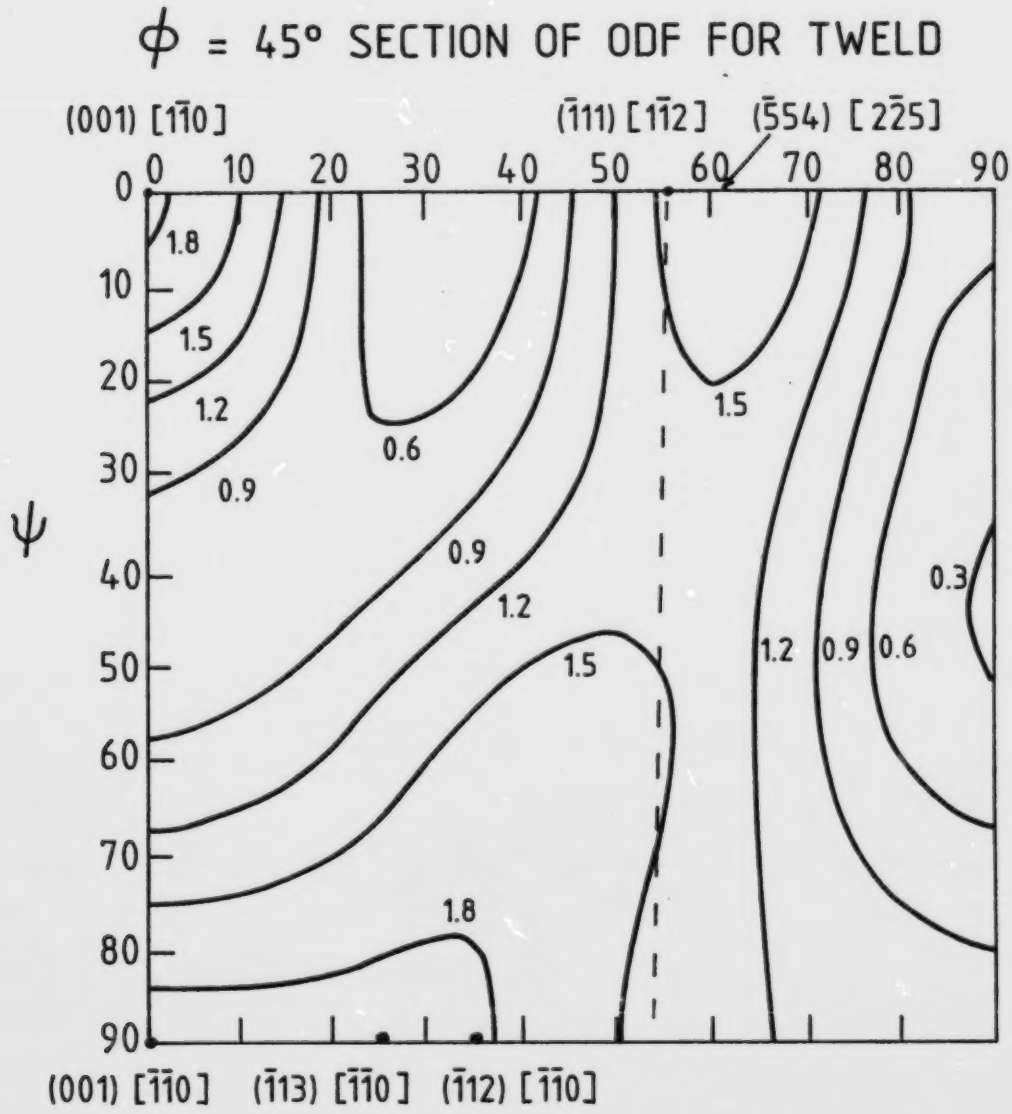

Fig. 7. ϕ = 45° section of the orientation distribution function for the T-weld sample. The texture includes the [110] fibre axis along the bottom of the figure and a (111) axis along the dashed line. Several particular crystal orientations are indicated. Contours are labelled by the factor by which the grain orientation departs from a random orientation.

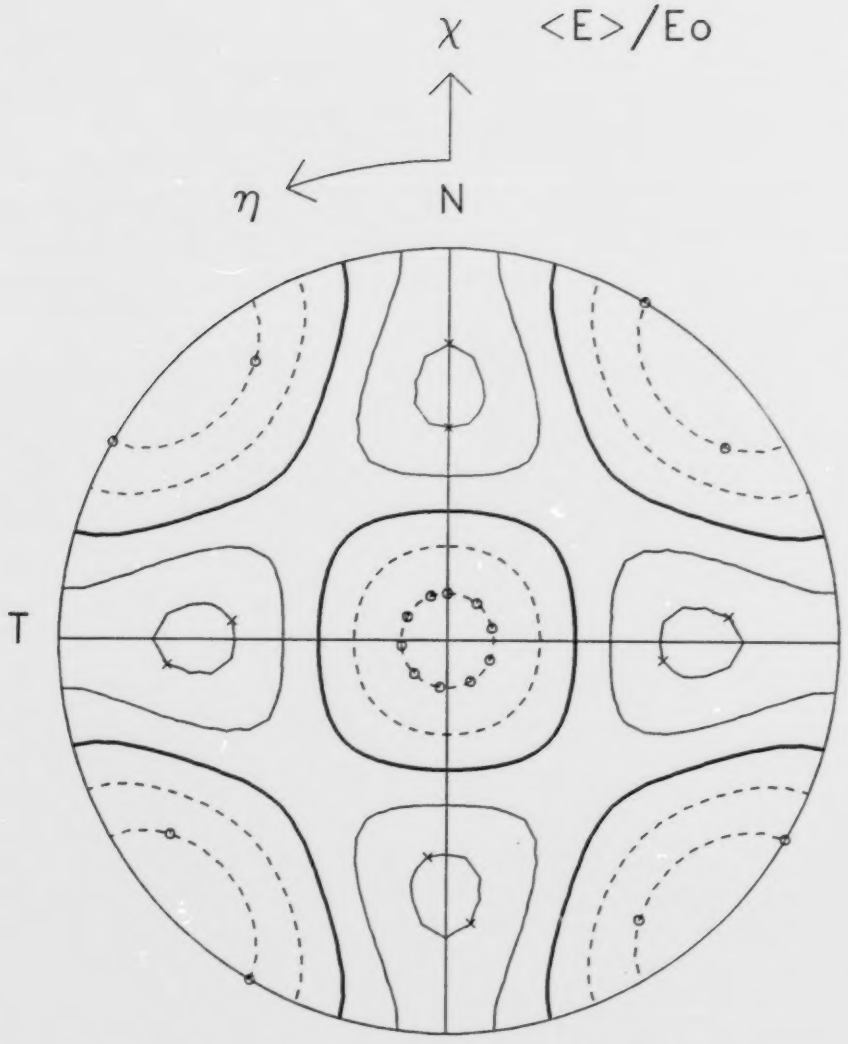

Fig. 8. Variation of the effective value of Young's modulus for the weld metal taken from the single-pass weld with orientation in a pole figure representation. The heavy lines denote the polycrystalline average Young's modulus for a texture free sample. Solid lines indicate increasing Young's modulus with a contour interval of 5% of the average, while dashed lines indicate decreasing Young's modulus.

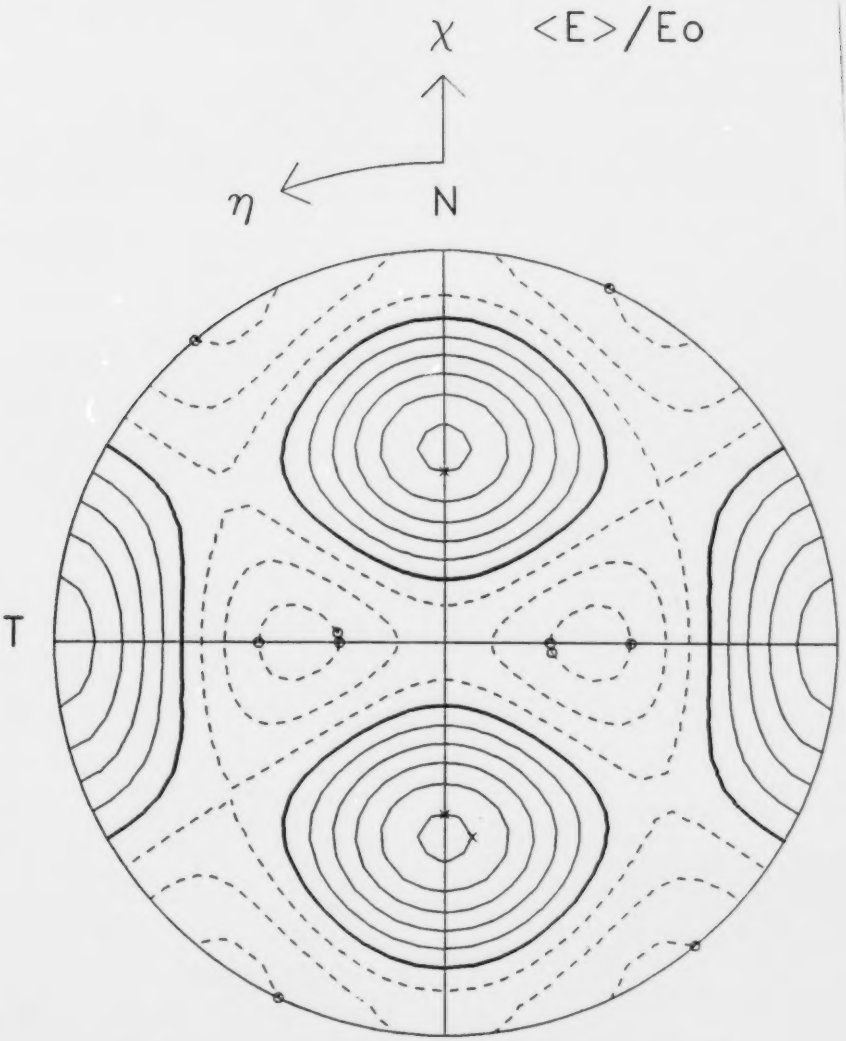

Fig. 9. Variation of the effective value of Young's modulus for the sample taken from the stainless steel plate in a pole figure representation. The heavy lines denote the polycrystalline average Young's modulus for a texture-free sample. Solid lines indicate increasing Young's modulus with a contour interval of 0.2% of the average, while dashed lines indicate decreasing Young's modulus.

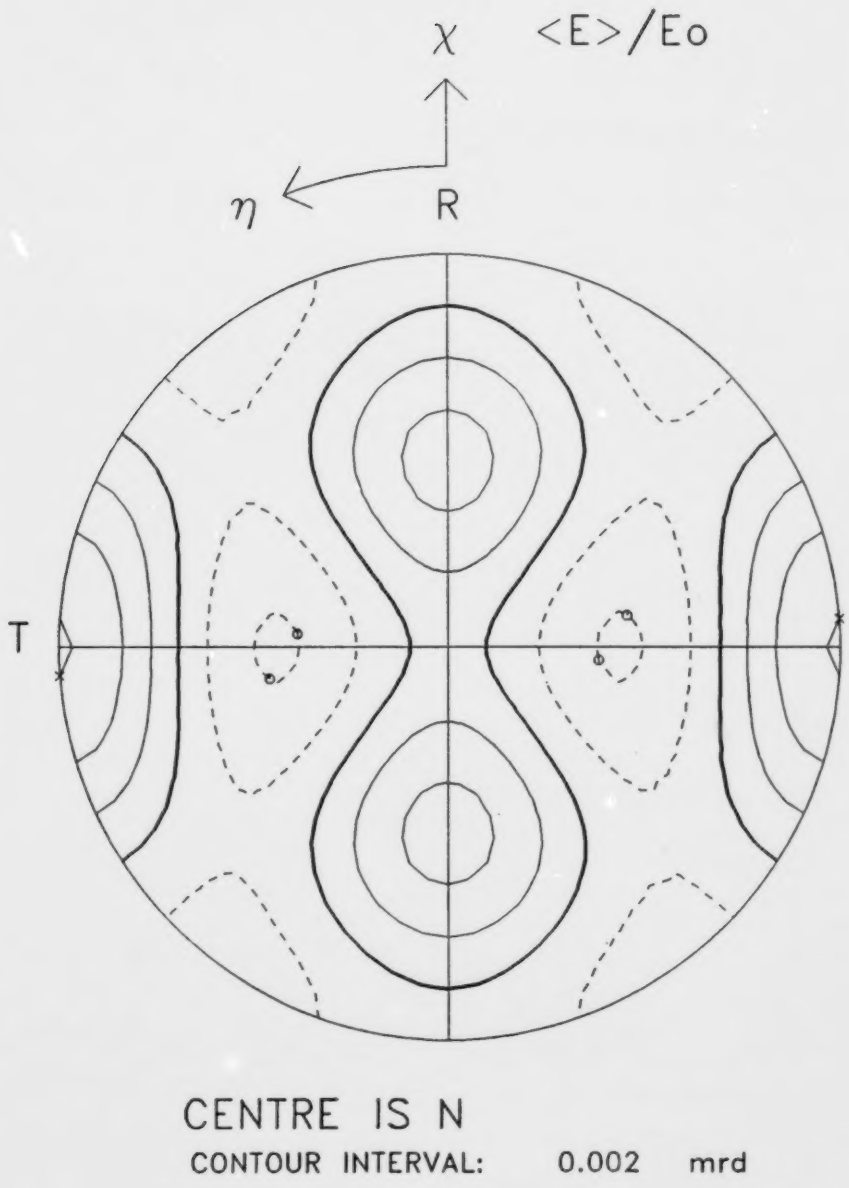

Fig. 10. Variation of the effective value of Young's modulus for the construction material of the T-weld in a pole figure representation. The heavy lines denote the polycrystalline average for a texture-free sample. Solid lines indicate increasing Young's modulus with a contour interval of 0.2% of the average, while dashed lines indicate decreasing Young's modulus.